JOINT INSTITUTE FOR NUCLEAR RESEARCH
Flerov Laboratory of Nuclear Reactions

FINAL REPORT ON THE INTEREST PROGRAMME

Production and spectroscopic investigation of new neutron-rich isotopes near the neutron N=126 shell closure using the multinucleon transfer reactions

Supervisor:
Mr. Viacheslav Vedeneev

Student:
Shota Amano, Japan
Kindai University

Participation period:
May 24 – July 02, Wave 4

Dubna, 2021

Introduction

The production of new superheavy elements and more neutron-rich nuclei is very important in the study of the origin of elements existing in the universe and the chemical evolution of the universe. However, there is the background that the cross section of such elements is becoming sharply decrease with conventional methods like the hot fusion reactions, the cold fusion reactions, and the fission reactions. As this reason, it is indispensable to propose the new method and elucidate the reaction mechanism in the future. Therefore, it is very important to investigate the shell effect of superheavy nuclei and neutron-rich nuclei. Since the shell effect is related to the survival probability of excited nuclei, it is also greatly related to whether it has synthesized superheavy nuclei and neutron-rich nuclei. The study of the nuclear shell structure leads to the reaching for the Island of Stability. It is interesting how the shell effect changes in more neutron-rich nuclei. In recent years, new methods using multinucleon transfer reactions have been proposed to synthesize new superheavy elements and neutron-rich nuclei [1-3]. The multinucleon transfer reactions have an advantage to enable to produce the variety of nuclides at one time, but the efficient collection and separation is required to identify the nuclides produced by this reaction method.

In this paper, the isotopes synthesized from the experimental data of the alpha spectrum measured by MASHA setup [4-7] are identified and the analysis results are reported. The analyzed reaction system is real data of $^{40}Ar+^{148}Sm$ and $^{40}Ar+^{166}Er$ complete fusion reaction and $^{48}Ca+^{242}Pu$ multinucleon transfer reactions.

Installation and main parts

The hot catcher represents a thermally expanded graphite foil. The reaction product (neutron evaporation residue) is released from the target with high energy, making analysis impossible. For these reasons, methodical online implementation of isotope separation. First, the reaction product is separated from the ion beam. Second, the required product is cooled and stops inside the solid carbon catcher. The stop ions fill the electron orbit, thus recombine, diffuse from the catcher, heat up to a very high temperature, and are transported to the ECR ion source, where they are ionized into +1 charged state, where the secondary beam is via a magnetic mass separator. Here the looseness of the atoms is very high, the measurement efficiency of the solid ISOL method is about 7% and the transport time reaches 2 seconds, which can be unsuitable for measuring the properties of isotopes in a short time.

Next, the position-sensitive strip detector is described. Each strip is an electrically isolated silicon detector with the width of 1.25 mm in the focal plane. When the nucleus sits on the surface of the detector, it begins to collapse on all 4π spheres. To cover as much space as possible, the detector configuration is well typed with focal and side/lateral crystals. This type of detector can detect alpha particles and fragments suitable for neutron-deficient alpha active nuclei. Neutron-rich nuclei mainly use TIMEPIX pixel detectors that decay in β-minus mode and can be placed in chambers except for one of the strip detector crystals. It represents an all-in-box with a sensitive area of 14*14 mm consisting of 256*256 pixels and can be used as a tracking 2-dimentional detector.

For the projectile ^{40}Ar of ^{48}Ca are usually used, because of the magic numbers of them and its spherical shape. Sphericity eliminates the orientation correction and yields of

these newborn nuclei products will be constant. Mercury is chosen as the homologist of elements Cn and Fl, which are supposed to be volatile metals at normal conditions. Mercury could sit on a wall of bare stainless steel where is colder places (potential hollow) and make strong compound with metals like amalgam. Thus, much of nuclei is missing; and if yields of mercury in these reactions is quite high, it is inappropriate to miss Cn. Radon is inert radioactive gas, so does not make any combinations with any of materials.

The experiment in the reaction of $^{48}Ca+^{242}Pu$ is performed as the multinuclear transfer reactions. Prior to that, all reactions were a complete fusion, the incoming ion strikes were central, the target parameter was zero, and all the nucleons participated in the reaction. Often, some targeted parameters and reaction films held at some of the nucleons will participate. Frequent observations are that the nuclei rotate after a strike, emitting some nuclei on at a wide angle. Instead of the complete fusion reaction, the product is released forward at the narrow solid angle, almost all of which can be caught by a graphite catcher, and in a multinuclear transfer reaction this angle is very large, 2π. In this case, the target + hot catcher composition is used. It can catch more nuclei and heat up.

TIMEPIX detectors are used for other types of radiation other than alpha and fragment. Normally, in the multinuclear transfer reactions, neutron-rich nuclei near N = 126 neutron shell closure are produced and decay mainly in β mode. The pixel detector is able to see the beta track. TIMEPIX cold detection also detects alpha, fragment, beta, gamma and X-rays over a wide energy range.

Project goals

The goal of this project is to analyze the α decay nuclei near the closed shell of N = 126 detected by the focal plane detector of the mass separator. First, the mass numbers of isotopes and the decay scheme are specified from the experimental data obtained from the complete fusion reactions neutron evaporation residues of $^{40}Ar+^{148}Sm$ and $^{40}Ar+^{166}Er$. The final goal of the project is to identify the exact alpha decay energy from the alpha spectra of the radon isotopes detected in the multinucleon transfer reactions of $^{48}Ca + ^{242}Pu$, and to identify the mass number of the isotope near the closed shell of N = 126 and the decay scheme.

Scope of work

During the work an accurate alpha decay energy and the alpha branching ratio of isotopes were defined, using the chart of nuclear and the experimental values of the detected simple alpha spectra by the single strip of a well-type detector in the reactions of $^{40}Ar+^{148}Sm$ and $^{40}Ar+^{166}Er$.

Based on that information, detector calibration was performed for each reaction to identify the alpha decay energy for each isotope. The same work was performed using the experimental data of the multinucleon transfer reactions $^{48}Ca+^{242}Pu$, and the alpha and beta decay nuclei were analyzed.

Methods

Open the experimental values in origin software and create a Step line graph with the x-

axis as Energy and the y-axis as Counts like Fig. 1. Find the peak and find its X coordinate value. This value is the temporary alpha decay energy.
Using the chart of nuclides showed Fig. 2, identify decay nucleus, and redefine temporary alpha decay energy as the exact energy.
Define energy peaks of all isotopes, mark them, and write down the exact isotopes, their decay energies, and the alpha branching ratios. Figure 3 is showed the exact decay nucleus and energy.
Next, open the experimental values of two-dimensional alpha decay energy-strip number and create a matrix. The alpha decay energy (E_alp.dec.) is selected from the one-dimensional simple alpha spectra of two different isotopes. Write down the Y-axis value * A * that indicates the position of the largest matrix, create the 2-dot linear equation *E_alp.dec.=Ax+B* found in the two unknowns, solve it and find * A * and * B *. This equation is used to recalibrate the Y-axis of the matrix. After getting the coefficients, rescale Y-axis using *Ax+B* This Y-axis value indicates the recalibrated alpha decay energy. Figure 4 shows the result after recalibration. It also identifies the isotopes detected. Other data in the reaction system of ^{40}Ar+^{166}Er and ^{48}Ca+^{242}Pu is also processed in the same way.

Figures

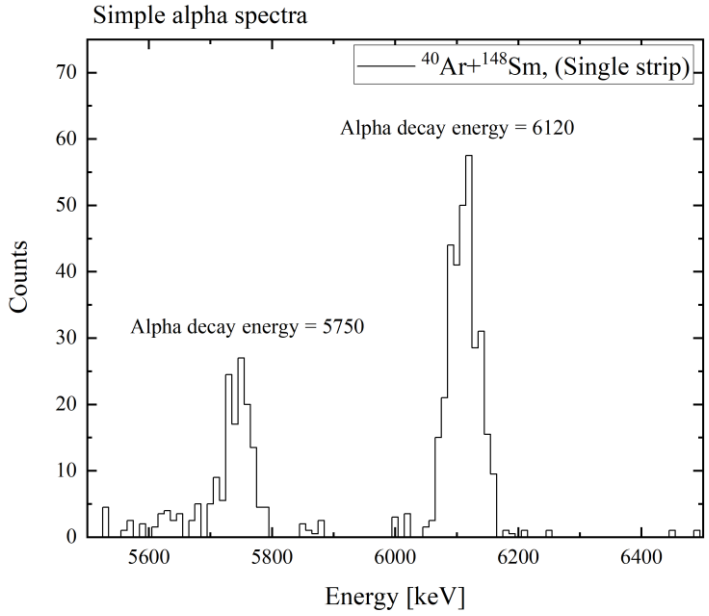

Fig. 1. The experimental data for simple alpha spectra. Alpha decay energy indicates X coordinate value.

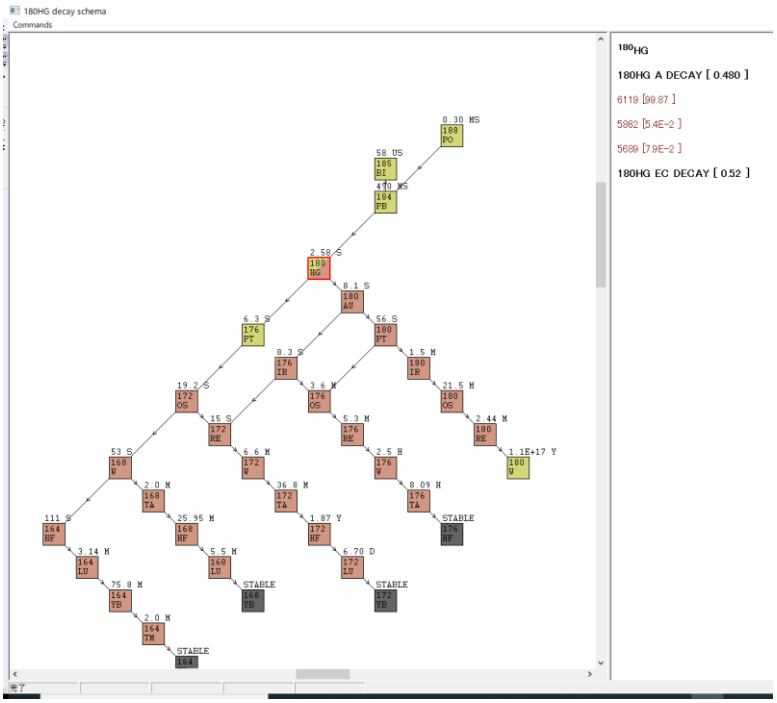

Fig. 2. The decay scheme for ^{180}Hg. Alpha decay energy is 6119 keV and alpha branching ratio indicates 99.87%.

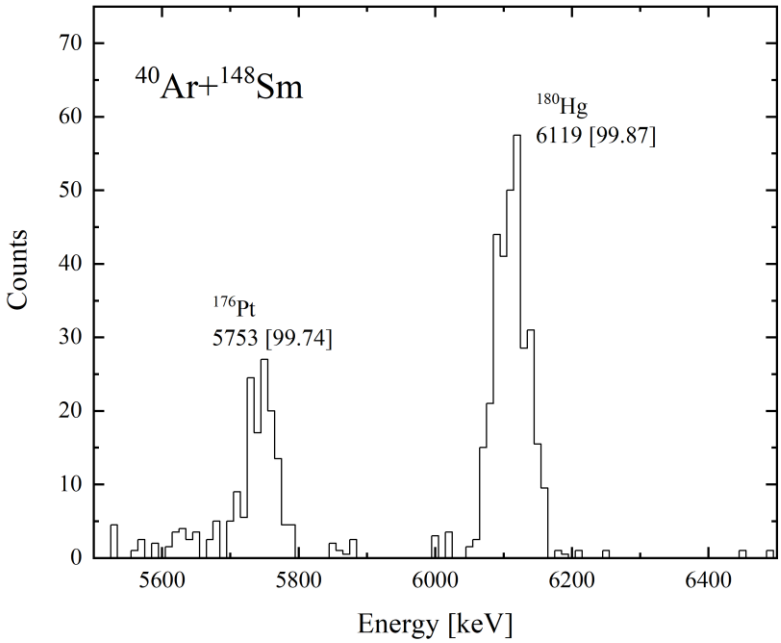

Fig. 3. The experimental data is alpha decay energy and alpha branching ratio for defined as the exact nucleus and include their of daughter nuclei decay.

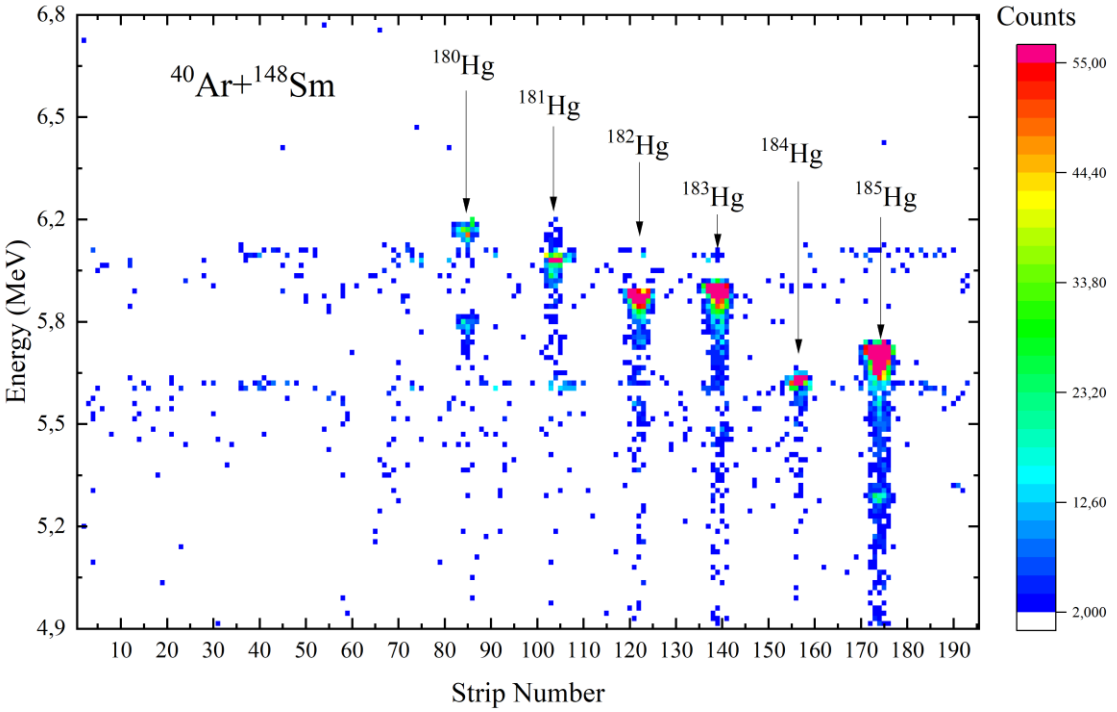

Fig. 4. Example of two-dimensional alpha decay energy-strip number in ^{40}Ar+^{148}Sm.

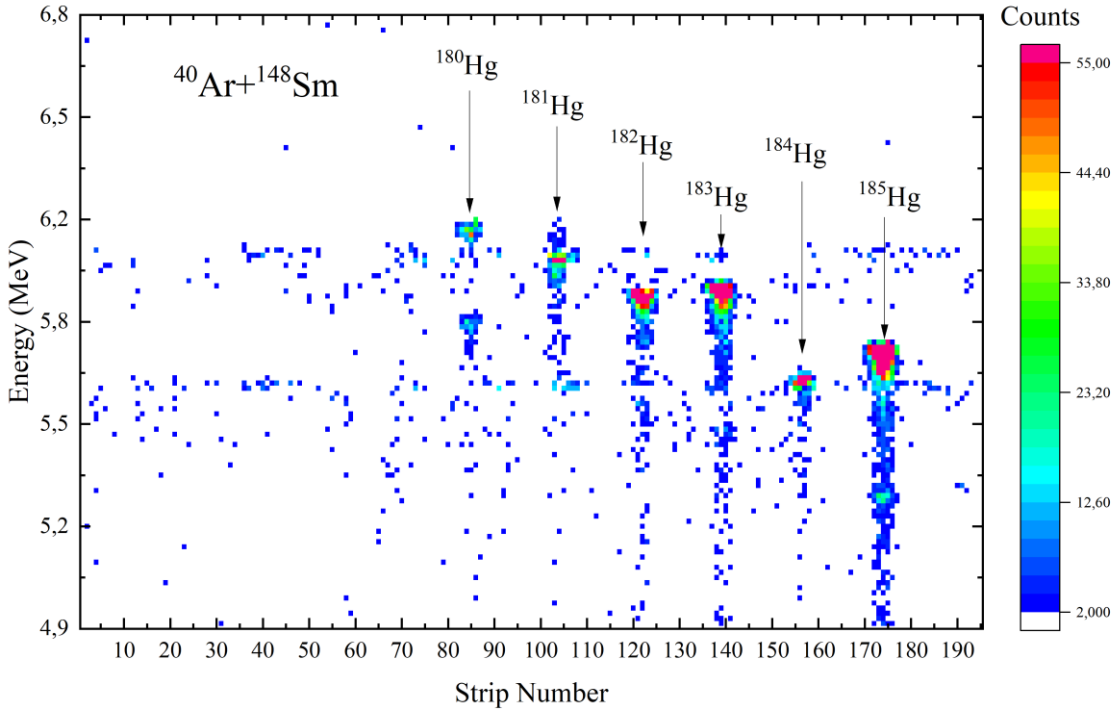

Fig. 5. Two-dimensional alpha decay energy-strip number for $^{180\text{-}185}$Hg isotopes in the reaction of ^{40}Ar+^{148}Sm.

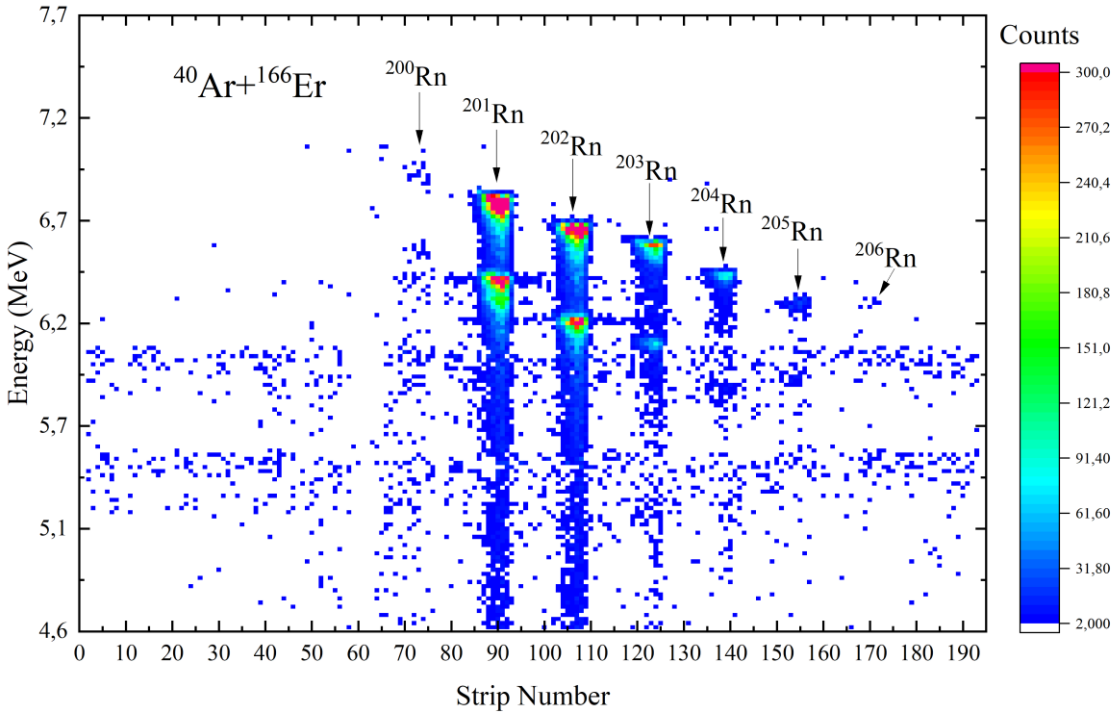

Fig. 6. Two-dimensional alpha decay energy-strip number for $^{200\text{-}206}$Rn isotopes in the reaction of ^{40}Ar+^{166}Er.

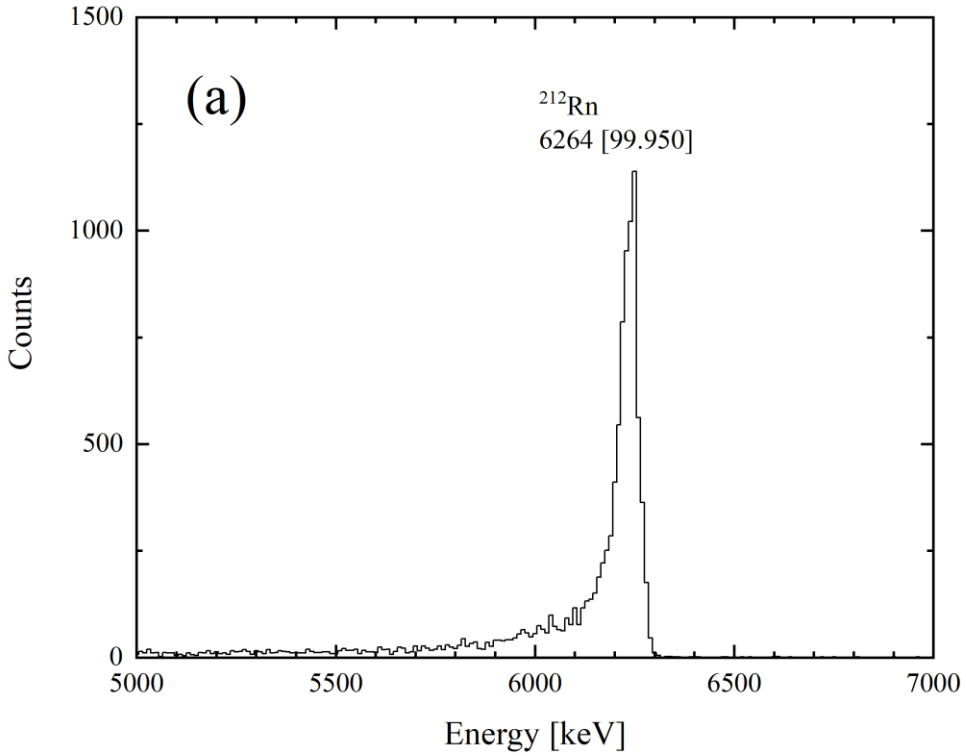

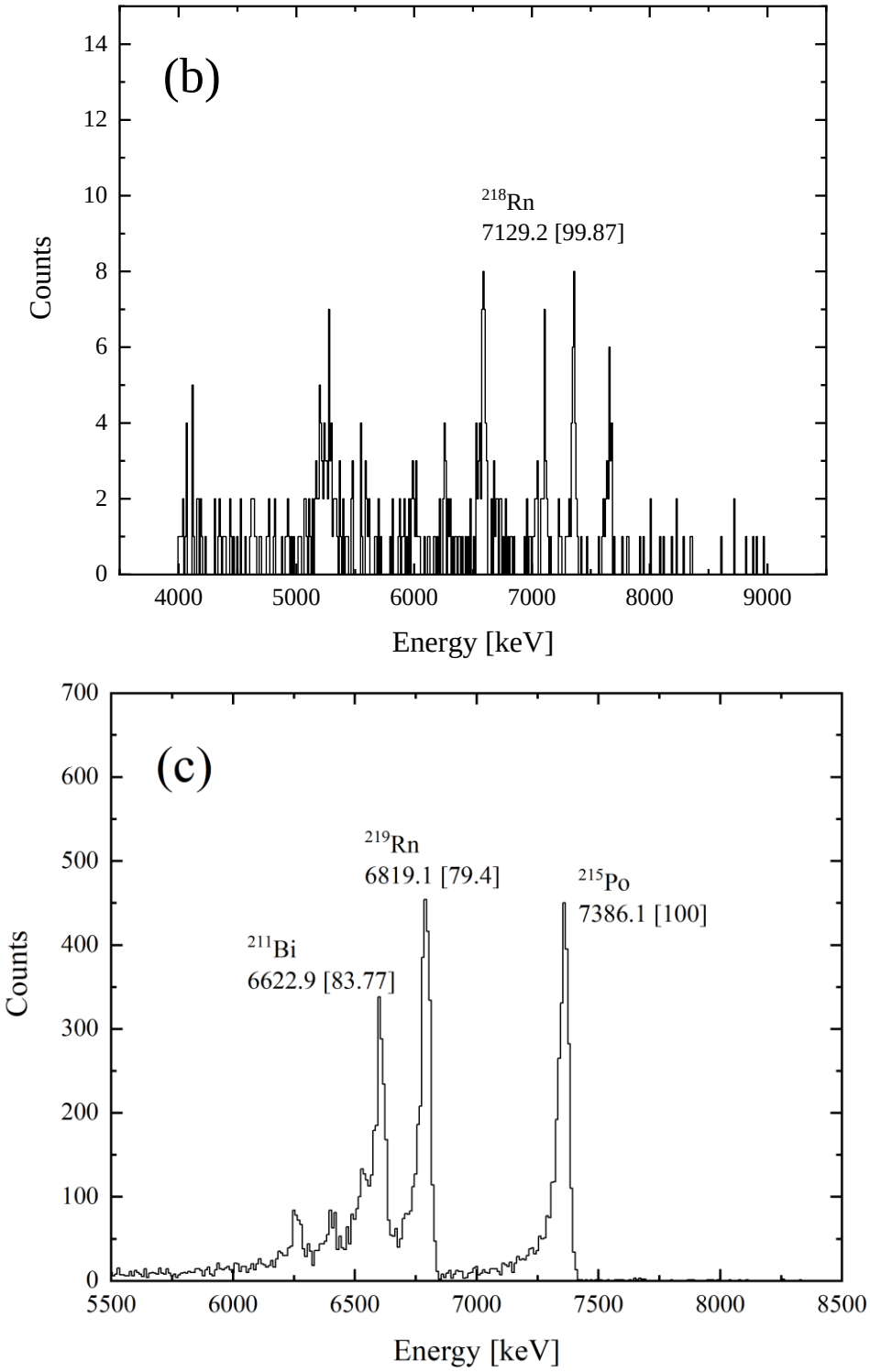

Figs. 7. The experimental value of Single alpha decay spectra defined as a) ^{212}Rn, b) ^{218}Rn and c) ^{219}Rn respectively.

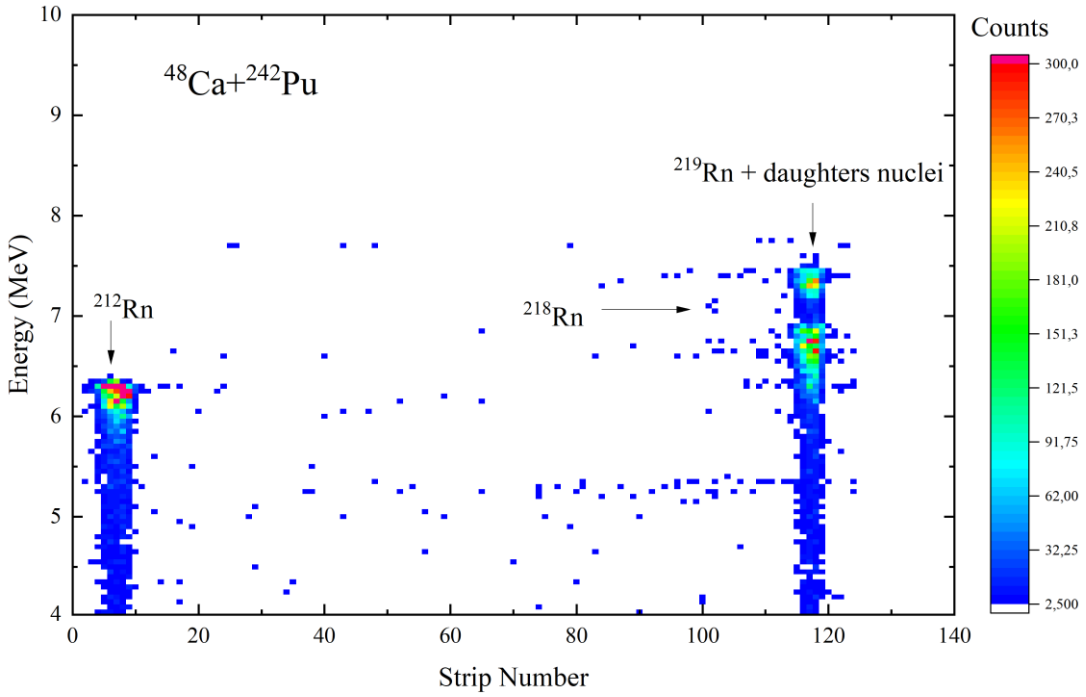

Fig. 8. Two-dimensional alpha decay energy-strip number for radon isotopes in the reaction of ^{48}Ca+^{242}Pu.

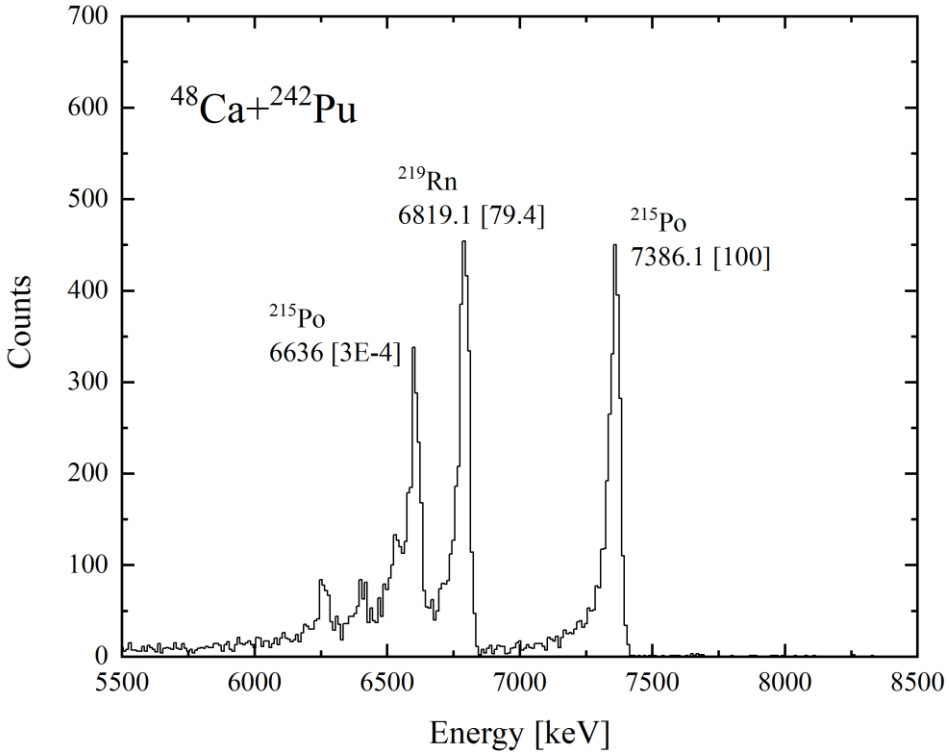

Fig. 9. The experimental value of Single alpha decay spectra defined as ^{219}Rn. The nuclide identified from the third energy peak shows ^{215}Po.

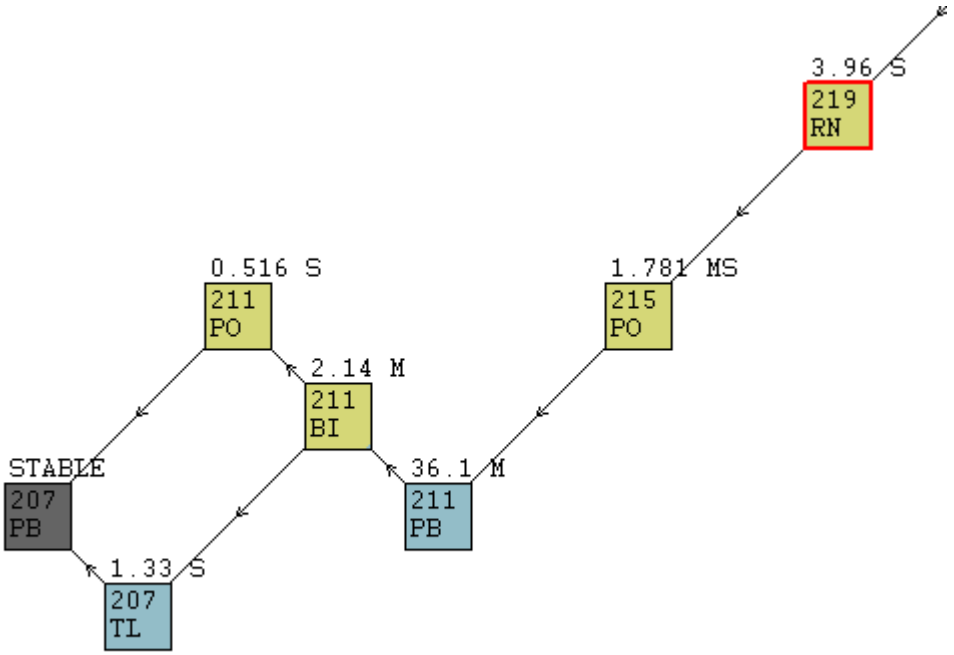

Fig. 10. Decay scheme of 219 radon.

Results

Figure 5 shows the two-dimensional alpha decay energy-strip numbers of 180-185 mercury isotopes carried out the detector calibration in the $^{40}Ar+^{148}Sm$ reaction system. The mercury isotopes produced by the complete fusion reaction of $^{40}Ar+^{148}Sm$ are clearly detected from 180 to 185. Figure 6 shows the two-dimensional alpha decay energy-strip number of 200-206 radon isotopes that performed detector calibration in the $^{40}Ar+^{146}Er$ reaction system. This graph shows that the radon isotopes produced by the complete fusion reaction of $^{40}Ar+^{146}Er$ are clearly present from 200 to 205. ^{206}Rn is almost invisible but exists. Next, the experimental data measured in the $^{48}Ca+^{242}Pu$ reaction system using the multinucleon transfer reaction will be analyzed. Figures 7(a)(b)(c) show the simple alpha spectrums of neutron-rich radon isotopes measured in the $^{48}Ca+^{242}Pu$ reaction system. In Fig. 7(a), it was identified that the energy peak was ^{212}Rn, which shows alpha decay energy and alpha branching ratio of 6264 keV and 99.950%, respectively. In Fig. 7(b), the energy peak is ^{218}Rn, which shows alpha decay energy and alpha branching ratio of 7129.2 keV and 99.87%, respectively. In Fig. 7(c), three energy peaks were confirmed. It was identified that the highest energy spectrum is ^{219}Rn, which shows the alpha decay energy and the alpha branching ratio of 6819.1 keV and 79.4%, respectively. The remaining two energy peaks are detected as alpha decay energy of the daughter nucleus. One of the energy peaks is ^{215}Po, which shows the alpha decay energy and the alpha branching ratio of 7386.1 keV and 100%, respectively. The other energy peak is the daughter nucleus ^{211}Bi with the alpha decay energy and the alpha branching ratio of 6622.9 keV and 83.77%, respectively. Figure 8 shows the two-dimensional alpha decay energy-strip numbers of the 212-219 radon isotopes that have performed the calibration of detectors using the data from one-dimensional histograms. ^{212}Rn and ^{219}Rn are clearly detected. ^{218}Rn is faintly visible. Radon isotopes with mass numbers from 213 to 217 are not almost detected. This is because they are smaller than the half-life of ^{218}Rn (35 ms). They decay before reaching the focal plane.

Conclusions

By analyzing the experimental data and performing calibration, the isotopes produced by the complete fusion reaction of ^{40}Ar+^{148}Sm and ^{40}Ar+^{146}Er and the multinucleon transfer reactions of ^{48}Ca+^{242}Pu were identified. In this work, ^{212}Rn shown N=126 closed shell is clearly identified and found to exist it, using multinucleon transfer reactions in MASHA setup. The alpha decay energy spectrum of ^{48}Ca+^{242}Pu shown in Fig. 9 is the same as that of Fig. 7(c), but the decay nuclei identified from the alpha energy are different. In the first analysis, the third peak has been analyzed as ^{215}Po with the alpha decay energy of 6636 keV and the alpha branching ratio of 0.0003%. However, the alpha branching ratio was too low for this peak, and the β- decay of the daughter nucleus ^{211}Pb after the alpha decay of ^{215}Po resulted in the alpha decay energy of 6622.9 keV and the alpha branching ratio 83.77% of ^{211}Bi. Therefore, it was concluded that ^{211}Bi was detected as the spectrum. ^{219}Rn undergoes three α decays and two β- decays,

$$^{219}\mathrm{Rn} \xrightarrow{\alpha} {}^{215}\mathrm{Po} \xrightarrow{\alpha} {}^{211}\mathrm{Pb} \xrightarrow{\beta^-} {}^{211}\mathrm{Bi} \xrightarrow{\alpha} {}^{207}\mathrm{Tl} \xrightarrow{\beta^-} {}^{207}\mathrm{Pb}$$

up to ^{207}Pb of stable nuclei. This decay scheme is shown in Fig. 10. In the future, we will carry out experiments to produce more neutron-rich nuclei by using the multinucleon transfer reactions and identify the detected isotopes to clarify the nuclear shell structure in that region.

References

1. V. I. Zagrebaev and W. Greiner, Phys. Rev. Lett., 2008, vol. 101, p. 122701.
2. A.V. Karpov and V. V. Saiko, Phys. Rev. C, 2017, vol. 96, p. 024618.
3. V. I. Zagrebaev, Yu. Ts. Oganessian, M. G. Itkis and W. Greiner, Phys. Rev. C, 2008, vol. 73, p. 122701.
4. V. Yu. Vedeneev, et al. The current status of the MASHA setup. Hyperfine Interactions, 2017, 238.1: 19.
5. E. V. Chernysheva, et al. Determination of Separation Efficiency of the Mass-Spectrometer MASHA by Means of Measurement of Absolute Cross-Sections of Evaporation Residues. In: Exotic Nuclei: Proceedings of the International Symposium on Exotic Nuclei. 2020. p. 386-390.
6. A. M. Rodin, et al. Features of the Solid-State ISOL Method for Fusion Evaporation Reactions Induced by Heavy Ions. In: Exotic Nuclei: Proceedings of the International Symposium on Exotic Nuclei. 2020. p. 437-443.
7. A. M. Rodin, et al. MASHA separator on the heavy ion beam for determining masses and nuclear physical properties of isotopes of heavy and superheavy elements. Instruments and Experimental Techniques, 2014, 57.4: 386-393.

Acknowledgments

The author would like to thank INTEREST team of Joint Institute for Nuclear Research University Centre for providing me an opportunity to participate in Wave 4 online program. The author also would like to thank Mr. Viacheslav Vedeneev of this project supervisor belonging the FLNR for his various advice. The graphs had carried out with Origin pro software ver. 2020b for Lightstone Corp.